

Analysis of the Gearing–Antigearing Torsional Fundamental Energy Gap in Dimethyl Ether[†]

Vojislava Pophristic[‡] and Lionel Goodman^{*}

Wright and Rieman Chemistry Laboratories, Rutgers, The State University of New Jersey, New Brunswick, New Jersey 08903

Received: October 11, 2002; In Final Form: January 23, 2003

Bimethyl rotor molecules, e.g., dimethyl ether (DME) exhibit two kinds of torsion: gearing (rotors turning out-of-phase) and antigearing (rotors turning in-phase). Although it is widely accepted that the fundamental frequencies of these two motions frequently differ by several tens of cm^{-1} , no systematic study of the physical origin of this splitting has been given. We report a series of dimethyl ether gearing/antigearing fundamental frequency splitting calculations where separate consideration of exchange repulsion, delocalization (hyperconjugation) interactions, and nonrotational phase space of the torsional coordinate indicate that the splitting is largely due to hyperconjugation between CH bonds of the two methyl groups. There is an inference that CH bond hyperconjugation is a major cause of the splitting in bimethyl rotor molecules, in general.

I. Introduction

The problem that we consider in this paper is the frequency difference between the a_2 (“antigearing”) and b_1 (“gearing”) simultaneous rotation fundamental torsional modes of the two methyl groups of a bimethyl molecule.¹ The calculated and observed splitting magnitudes generally are several tens of wavenumbers, even for those cases where the methyl groups are quite separated.² While there have been a number of ab initio studies with calculation of the torsional frequencies as their goal,^{3,4} our focus is on the intramolecular interactions controlling the gearing/antigearing fundamental frequency difference. It is quite surprising that this basic issue is not as yet better comprehended. Understanding the origin of this difference is particularly apropos because recent studies have indicated that steric repulsion interactions do not provide a satisfactory explanation for the structural preference of such small molecules as ethane and methanol.^{5,6}

Dimethyl ether (DME) is our molecule of choice for investigating the splitting origin (Figure 1). DME is one of the simplest molecules with two methyl torsional tops, and consequently it has the potential to serve as a benchmark molecule for obtaining an understanding of the interactions involving coupled methyl rotors. An extensive calculation of the potential energy hypersurface, which considers perturbations of the torsional levels by resonance interactions with the bending mode, has been carried out by Senent, Moule, and Smeyers.⁷ Although no experimental measurement of either the torsional fundamental ordering or the gap exists for DME, all ab initio calculations, no matter at what level, generate a gearing > antigearing ordering with $\sim 40 \text{ cm}^{-1}$ frequency difference.^{8–10}

From a repulsion model point of view, the gearing > antigearing fundamental sequence seems intuitive. Gearing motion involves close approach (“clashing”) of the $\text{C}_a\text{--H}_1$ and

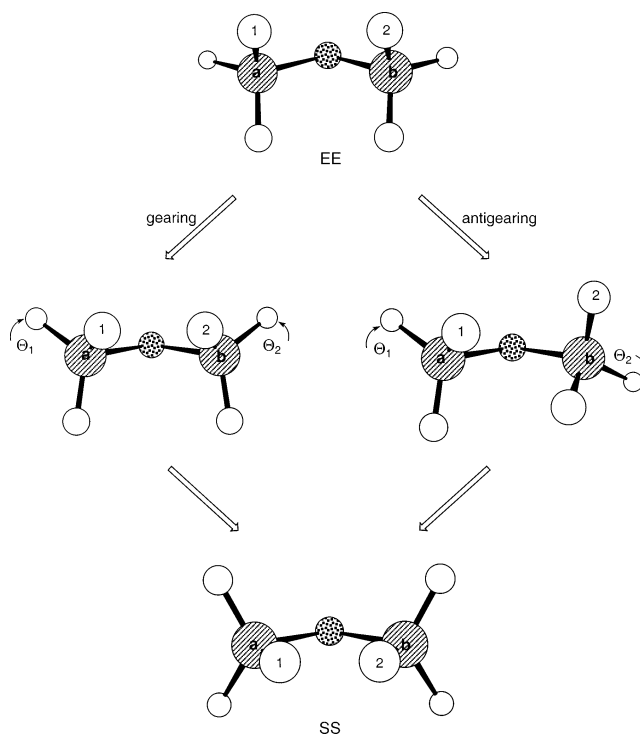


Figure 1. Dimethyl ether internal rotation from the equilibrium (EE) to the top-of-barrier (SS) conformer. The b_1 symmetry gearing rotation occurs as an out-of-phase motion, a_2 symmetry antigearing as an in-phase motion.

$\text{C}_b\text{--H}_2$ bonds of the methyl tops. The increased repulsion generates a steeper gearing potential well with consequently higher fundamental frequency than that for antigearing motion, where the rotors “avoid” each other. Gearing > antigearing frequency ordering is a well known phenomenon exhibited by a number of dimethyl molecules.¹¹

The traditional approach to double-rotor potential surfaces for skeletally planar C_{2v} molecules is in terms of a Fourier expansion appropriate to C_{3v} rigidly rotating methyl tops:

[†] Part of the special issue “George S. Hammond & Michael Kasha Festschrift”.

^{*} Corresponding author.

[‡] Present address: Department of Chemistry, University of Pennsylvania, Philadelphia, PA 19104.

TABLE 1: MP2/6-311G(3df,2p) Optimized Geometries of Equilibrium (EE) and Top-of-Barrier (SS) Conformers (bond lengths in Å, bond angles in degrees)

	C–O	C–H _{ip} ^a	C–H _{op} ^a	∠COC	∠H _{ip} CO ^a	∠H _{op} CO ^a
EE	1.405	1.086	1.095	111.3	107.5	111.4
SS	1.409	1.092	1.091	116.9	111.9	109.8

^a H_{ip}, H_{op} refer to in-plane and out-of-plane hydrogen atoms.

$$\Delta V(\Theta_1, \Theta_2) = \frac{1}{2}V_3(\cos 3\Theta_1 + \cos 3\Theta_2) + \frac{1}{2}V_{33} \cos 3\Theta_1 \cos 3\Theta_2 + \frac{1}{2}V'_{33} \sin 3\Theta_1 \sin 3\Theta_2 + \frac{1}{2}V_6(\cos 6\Theta_1 + \cos 6\Theta_2) \quad (1)$$

where Θ_1 and Θ_2 are torsional angles of the two methyl groups defined as counterclockwise rotation looked at from the oxygen atom (Figure 1), and $\Delta V(\Theta_1, \Theta_2)$ is the energy of the Θ_1, Θ_2 conformer relative to the equilibrium one. The torsional frequencies are obtained by solving the C_{3v} rigid rotor Mathieu equation¹² in terms of the Hamiltonian function

$$\mathcal{H} = F(p_1^2 + p_2^2) + F'(p_1 p_2 + p_2 p_1) + V(\Theta_1, \Theta_2) \quad (2)$$

In eq 2, $p_i = -i\partial/\partial\Theta_i$ is the conjugate momentum associated with methyl top rotation, and F, F' are torsional kinetic energy coefficients, expressed in terms of moments of inertia of one rotor about its symmetry axis and about the molecular principal axes. An additional restriction is that the Hamiltonian in eq 2 neglects interactions between torsions and other vibrations. The C_{3v} symmetry condition required by eqs 1 and 2 is not strictly valid for DME (i.e., the HCH angles and C–H bond lengths are unequal, Table 1), and the phase space of the methyl torsional coordinate includes COC angular motion.^{10,13} However, frequency simulation studies using the C_{3v} condition show reasonably good agreement (e.g., ref 8) with the experimentally observed infrared active b_1 frequency.¹⁴ In any case, our goal is not precise frequency simulation but rather physical understanding of the large gearing/antigearing frequency difference. For this purpose, Ockham's Razor is the approach of choice.

II. Potential Constant – Torsional Frequency Connections

The three cosine terms in eq 1 describe interactions of methyl rotors with the molecular frame and with each other, leaving the two torsional fundamental frequencies equal provided the F' kinetic coupling term in the Hamiltonian is neglected.^{15,16} This degeneracy is lifted by introducing the sine term, V_{33}' , which also includes methyl–methyl interactions. However, the degeneracy of the torsional fundamental vibration energies is also lifted by F' , which cannot be neglected in any discussion of the effect of the potential constants on the frequencies. Since F' (and F) are completely determined by molecular geometry we proceed by using $F = 6.74102$ and $F' = -1.20583$, calculated from the MP2/6-311G(3df,2p) optimized equilibrium conformer DME geometry, neglecting any torsional angle dependence. Use of the equilibrium geometry is justified by our focus on torsional fundamental energy levels, lying near the bottom of the torsional potential curves. The effects of the four potential constants and F' on the a_2 and b_1 torsional fundamental energy spacing are illustrated in Figure 2. Figure 2a shows the strong relationship between the spacing and the barrier height determining V_3 constant. While the barrier shape determining constant, V_{33} , has little effect on the fundamental

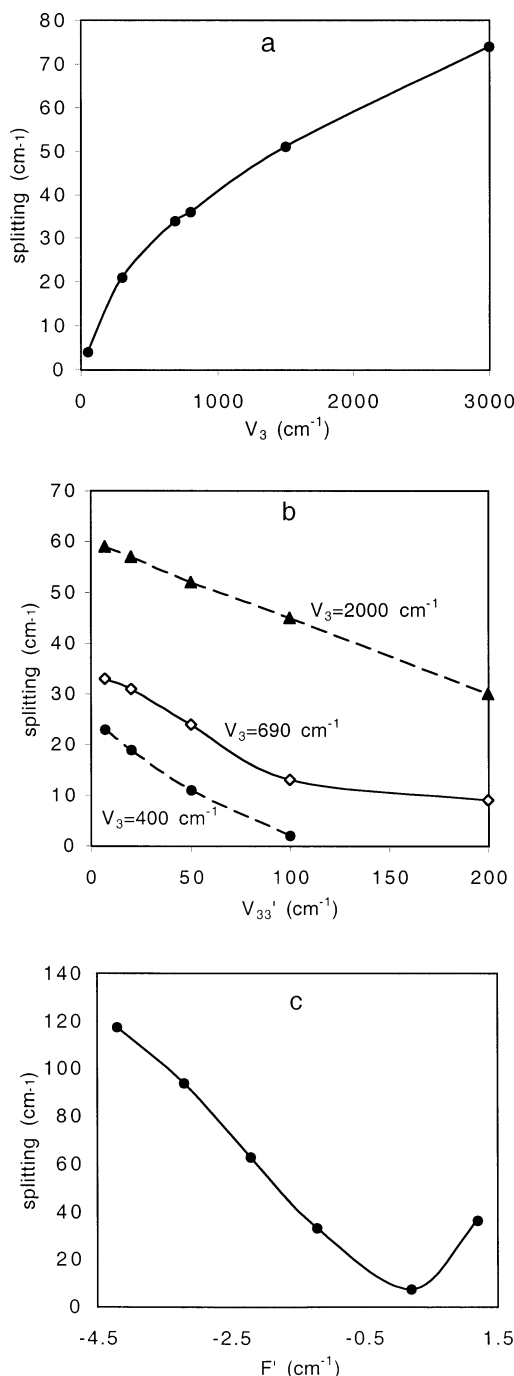


Figure 2. Potential constant–gearing–antigearing splitting connections. F and F' constants fixed as in text, except for (c). (a) V_3 variable, $V_{33} = V_{33}' = V_6 = 0$; (b) V_{33}' variable, $V_{33} = V_6 = 0$; (c) $V_3 = 690$ cm⁻¹, $V_{33} = -58$ cm⁻¹, $V_{33}' = 7$ cm⁻¹, $V_6 = 2$ cm⁻¹, $F = 6.74102$, from Table 2.

splittings, its effect on overtone and combination level splittings is substantial.¹⁷ When the signs of V_{33} and V_3 are opposite, as in the case of DME, the a_2 fundamental energy is the lower one,⁷ but the splitting is always decreased when $|V_{33}'|$ is increased, independent of the magnitude of V_3 (Figure 2b).

The sensitivity of the spacing to F' is shown in Figure 2c. The curves show that the spacing strongly depends on the F' – V_{33}' connection and that the 30–40 cm⁻¹ frequency separation in DME is tied to the sizeable F' constant. However, since F' is fixed by molecular geometry alone, our focus is on the potential constants, which ultimately are determined by the nature of the interactions.

TABLE 2: Torsional Potential Constants and Fundamental Frequencies for Real Dimethyl Ether, and Hypothetical Models Excluding Exchange and Delocalization Energies, (cm⁻¹)^a

	all interactions (present)	exchange repulsion (absent)	delocalization (absent)	ref 8 ^b
		potential constants		
V_3	690	3452	132	890
V_{33}	-58	-140	242	-101
V_{33}'	7	450	-139	43
V_6	2	344	1	17
		torsional frequencies		
antigearing (a_2) fundamental	179	492	36	204.7
gearing (b_1) fundamental	212	539	46	242.3 (241.0)
gearing/antigearing splitting	33	47	10	37.6

^a HF/6-311G(3df,2p) energy calculation; MP2/6-311G(3df,2p) geometry optimization. ^b Experimental result given in parentheses (ref 14).

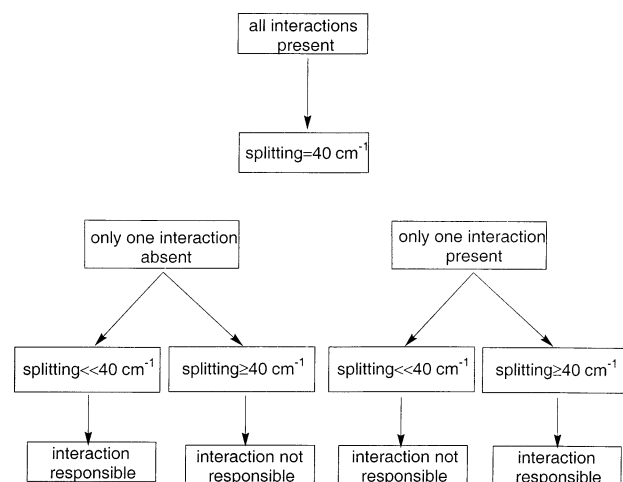


Figure 3. Schematic diagram showing calculational scenarios determining which interactions play roles in the torsional frequency splitting.

An illustration of the V_3 gearing/antigearing spacing connection is provided by comparing the torsional frequencies in free DME to those in a hydrogen bonding environment. Protonation of DME produces a flattening of the torsional potential curves (i.e., the magnitude of V_3 is decreased).⁹ This occurs because bonding of the lone pair in hydrogen bonding media leads to a much lowered barrier (~ 1 kcal/mol)^{9,18} reduced from the ~ 5 kcal/mol calculated for the free molecule. There is a consequent reduction in the calculated splitting (to 25 cm⁻¹), despite the counter effect engendered by the decreased magnitude of the V_{33}' constant.¹⁹

III. Plan

The parametric analysis given in section II, while useful in relating the gearing/antigearing fundamental splitting to rotational barrier features, does not give insight into the intramolecular interactions behind these features. An insightful approach to understanding internal rotation potential surfaces is to partition the energy into three factors: exchange repulsion, hyperconjugative interactions, and the energetic effect of skeletal changes that reduce the strain that is accumulated in the molecule by rotation alone.²⁰ This ansatz was successfully used to analyze ethane and methanol barrier heights.^{5,6}

The scheme adopted here is to determine the factors controlling the splitting of the gearing and antigearing fundamental frequencies by analyzing frequencies of hypothetical DME molecules, which lack the interaction under investigation.

Figure 3 illustrates how this scheme tests whether a specific interaction splits the a_2 and b_1 fundamental frequencies. If an interaction is excluded from the model, and the resulting fundamental frequency difference remains essentially the same

or is increased, then that particular interaction does not account for the splitting. In this case one or more of the other intramolecular forces, still present in the model, is responsible. If, on the other hand, the frequency difference vanishes or is greatly reduced, then the presence of that particular interaction forces the splitting. For each case of a specific interaction absent, a set of four V_i constants is computed using the same set of conformers (and consequently the same set of kinetic energy constants) as for the real molecule, and based on these V_i constants, torsional frequencies are derived.

Note should be taken that a second type of hypothetical molecule is possible, which has only one specific interaction present (also shown in Figure 3). While there is substantial evidence that meaningful potential surfaces arise from the first scheme,^{5,21} potential surfaces derived from the second scheme are more problematical and thus will only be used in a supporting role.

The energy analysis was performed within the Hartree Fock (HF) framework at the 6-311G(3df,2p) level using Natural Bond Orbital (NBO) 4.M²² and Gaussian 98 software.²³ Natural bond orbitals,²⁴ because of their localization in orthonormal bonds and antibonds, allow specific interactions to be pinpointed. Torsional frequencies were calculated using TACIR.²⁵ The resulting V_i constants and fundamental frequencies are listed in Table 2. Although HF predictions for both the a_2 and b_1 frequencies are somewhat too low as compared to MP2 predictions, we are interested in the origin of the a_2 - b_1 difference, which is largely preserved at the HF level of calculation (i.e., 33 cm⁻¹) compared to the 38 cm⁻¹ MP2 calculation⁸ and 41 cm⁻¹ for the most elaborate prediction.¹⁰ An additional rationale for the HF calculations is that the HF method, which even with modest basis sets predicts a reasonable torsion fundamental splitting, should correctly describe the physics of the splitting.

IV. Results

A. Exchange Repulsion. The antisymmetrization effect (basically the steric repulsion effect arising from the Pauli principle leading to a tendency of electrons to avoid occupying the same space) is determined in natural bond orbital theory as the energy difference between orthogonal (NBO) and nonorthogonal (preorthogonal, pNBO) wavefunction descriptions of a molecule.^{26,27} Thus, internal rotation potential curves with antisymmetrization absent have been obtained by calculating the pNBO energy for each dimethyl ether rotated conformer. From these calculated potential curves, we compute torsional energy levels for a hypothetical DME molecule with the steric effect missing.

Table 2 shows that removing antisymmetrization greatly increases the magnitude of all four potential constants in

TABLE 3: DME Internal Rotation Energetics (kcal/mol)^a

	ΔE
barrier	4.26
exchange repulsion	-16.49
delocalization	4.83
oxygen (σ) lone pair	18.23

^a HF/6-311G(3df,2p) energy calculation; MP2/6-311G(3df,2p) geometry optimization.

equation 1. The large increase in $|V_{33}|$ results in a much raised average frequency of the two fundamentals; however, the decreased splitting, caused by the large increase in V_{33}' , is counteracted by the increase in V_3 (see upper curve of Figure 2b). The consequence is that splitting between the gearing and antigearing frequencies is essentially preserved (i.e., slightly increased to 47 cm^{-1}), even if the exchange repulsion is absent. We conclude that steric crowding arising from exchange repulsion is not the interaction that can be identified with the 30–40 cm^{-1} splitting between the two torsional fundamental frequencies.

B. Hyperconjugation. Hyperconjugative or delocalization stabilization can be determined in NBO theory as the energy increase associated with deletion of low occupancy antibonds.²⁸ Thus, the delocalization energy of a particular conformer is obtained by removing all antibond (and Rydberg) orbitals from the orbital space and recalculating the SCF energy for the conformer with these orbitals absent. The remaining electron structure is the Lewis structure, with all the bonds, lone pairs, and core orbitals having exact 2.0 occupancies. This interaction strongly depends on the relative orientation of donor and acceptor orbitals. Unlike the exchange interaction, it has a barrier forming character in DME (Table 3), and therefore the internal rotation potential curves with hyperconjugation switched off are displaced from those of the real DME molecule – their maxima are at the EE geometry.

The potential curves, constructed with delocalization absent, yield antigearing and gearing frequencies (36 and 46 cm^{-1} , Table 2) with transparently greatly reduced splitting. It is clear from this result that hyperconjugative interactions are to a large extent responsible for the splitting between the DME gearing and antigearing fundamental frequencies. Note that these interactions also play an important role in the DME internal rotation barrier.¹⁸

C. Nonrotational Component of the Torsional Coordinate.

The effect on the fundamental frequencies by the nonrotational part of the torsional coordinates can be assessed by comparing rigid and fully relaxed rotation models for the torsional fundamental frequencies in DME. Rigid rotation, in effect, describes the torsional coordinates as pure rotation.

The fully relaxed barrier, calculated at ~ 5 kcal/mol, is increased to ~ 7 kcal/mol with concomitant increase in V_3 .⁸ The consequence is an increase in the gearing/antigearing splitting to ~ 70 cm^{-1} from the 40 cm^{-1} gap predicted by the fully relaxed model. There is a clear conclusion: the nonrotational component of the torsional vibration phase space significantly decreases the gearing/antigearing gap. We conclude that the skeletal motions accompanying methyl internal rotation in DME are not responsible for the adopted 40 cm^{-1} gap.

Additional insight into the composition of the two torsional modes can be obtained by deuterium frequency shifts. For pure harmonic rotations involving only hydrogen atoms, the gearing/antigearing gap should decrease by 29%. Substantial motion in the nonrotor region of the molecule will lead to only partial sampling of the rotational phase space, and both the frequencies and the gap will undergo a lesser decrease.

The 241.0 cm^{-1} experimentally determined IR b_1 torsional fundamental frequency undergoes a 21% shift to 188.6 cm^{-1} in the d_6 isotopomer of DME, compared to the 170 cm^{-1} expected for a pure harmonic rotation. The 19 cm^{-1} discrepancy is evidence that the b_1 torsion is imperfectly sampling the gearing potential surface. As mentioned in the Introduction, there are no experimental observations for the a_2 torsion. However, the ab initio fully relaxed model 194 cm^{-1} a_2 fundamental calculated frequency is predicted to shift by 27.4% to 141 cm^{-1} . This frequency is only slightly higher than 137 cm^{-1} for pure harmonic rotation.

The conclusion is that the a_2 torsion is close to pure rotation. There is spectroscopic evidence for coupling of the b_1 torsion overtone to the COC in-plane bending mode in DME- h_6 at 412.0 cm^{-1} . Senent, Moule, and Smeyers¹⁰ have discussed the complex mode couplings in DME in detail, including the resonance interactions with the bending mode.

V. Discussion

Although the three energetic factors given in the preceding section are not entirely independent, their analysis provides a clear conclusion: it is the decrease in hyperconjugation as rotation proceeds that provides the major link to the torsional splitting. This is not an entirely surprising result, considering the important role that this factor plays in the barrier mechanism for DME.¹³ The overarching question is to pinpoint the specific electron transfer(s) controlling the gearing/antigearing splitting. A second question concerns the conclusion that skeletal relaxation reduces the splitting. Again, the need is to pinpoint the specific relaxation(s) that reduce the calculated pure rotational splitting from ~ 70 cm^{-1} to the adopted 40 cm^{-1} value.

The largest single hyperconjugative interaction is between the methyl groups involving the in-plane σ_{CaH} bond in the EE conformer with the σ_{CbH}^* antibond of the other methyl.²⁹ The $\sigma_{\text{CaH}}-\sigma_{\text{CbH}}^*$ interaction is mainly controlled by changes in overlap of the back lobe of σ_{CaH} with the main lobe of σ_{CbH}^* . Gearing rotation decreases the delocalization energy due to this interaction gradually; antigearing more rapidly, because the $\sigma_{\text{CaH}}/\sigma_{\text{CbH}}^*$ overlap attenuates more abruptly as the σ_{CaH} and σ_{CbH}^* orbitals move closer to the less overlap-effective *anti* orientation.²⁰ There is a parallel to the decrease in $\sigma_{\text{CaH}}-\sigma_{\text{CbH}}^*$ overlap with consequent loss of delocalization energy found for ethane internal rotation.⁵

The hyperconjugative machinery described here provides a useful picture for the origin of gearing/antigearing gaps in bimethyl rotor molecules, in general. The implication is that large gearing/antigearing rotation gaps found for many bimethyl molecules (e.g., see ref 2) involve a similar electron-transfer mechanism between the methyl groups.

As shown in Table 1, the principal relaxations in DME are a nearly 5° opening of the COC angle and methyl group folding (expressed by opposite changes in the $H_{\text{ip}}\text{CO}$ and $H_{\text{op}}\text{CO}$ angles). The effect of COC angular opening alone is to substantially lower the rigid rotation barrier (by more than 1 kcal/mol).¹⁸ The combined effect of the COC angle opening and methyl folding closely reproduces the 4.4 kcal/mol calculated fully relaxed barrier.¹⁸

Methyl group folding appears to originate in methyl–methyl hyperconjugative interactions. The COC angle opening appears to mainly arise from two factors: methyl $\sigma_{\text{CaH}} \Rightarrow \sigma_{\text{OCb}}^*$ electron-transfer and the repulsion between the electron density on the oxygen and the C–O bonding pair.^{13,18} There is a link between the increased lone pair p character as the rotation proceeds and the increased COC angle.¹⁸

The increase in lone pair energy due to the increased p character is barrier forming, and thus scheme 2 (see section III) can be employed. Its effect is to yield a much larger splitting than the accepted 40 cm^{-1} , suggesting that in DME, lone pair reorganization is also involved in the splitting mechanism (recall that switching off hyperconjugation leaves a residual 10 cm^{-1} gearing/antigearing gap).

VI. Conclusions

The origin of the gearing/antigearing torsional fundamental splitting is found to be largely controlled by vicinal hyperconjugative interaction between CH bonds and antibonds of the methyl groups. There is a strong inference that a similar methyl–methyl interaction is responsible for gearing/antigearing splittings in bimethyl rotor molecules, in general. A smaller but still significant component of the DME splitting is proposed to arise from reorganization of the oxygen lone pair orbital as rotation proceeds. The impure rotational character of the b_1 torsion in DME is a significant factor in reducing the splitting from a much larger estimated pure rotation splitting. We do not find evidence for repulsive interaction between the methyl groups providing significant contribution to the splitting.

Acknowledgment. George Hammond was my (L.G.) physical organic chemistry professor, my first semester at Iowa State. Despite George's clear and insightful lectures, I achieved the only failing grade in my scientific life and a dressing down from George that straightened me out. Shortly thereafter I decided to become a theoretical chemist (thesis director: Harrison Shull)! I spent two postdoctoral years in Michael Kasha's lab. There I met among others, Enrico Clementi, Mostafa El-Sayed, Sean McGlynn, Eion McRae, Ian Ross, Stewart Strickler, and Ralph Becker. Many of the Tallahassee contacts have flourished, and the experience of having been exposed to Mike's thinking (e.g., the necessity of being correct need not derail the momentum of a good idea) has stuck with me to this day.

Financial support from NSF and computational support from the San Diego Supercomputer Center are gratefully acknowledged. We thank an anonymous referee for an insightful comment which improved the paper.

Note Added after ASAP. The title for Table 2 was corrected after ASAP posting. The paper was originally posted to the Web on 3/25/03. The corrected version was posted on 3/31/03.

References and Notes

(1) These symmetry designations are for the important C_{2v} case considered in this paper.

- (2) Some examples are: acetone, 47 cm^{-1} (observed); dimethyl ether, $35\text{--}41\text{ cm}^{-1}$ (calculated); isobutene, 28 cm^{-1} (calculated); thioacetone, 53 cm^{-1} (calculated); acetone *n*-radical cation, 60 cm^{-1} (calculated); *trans*-2-butene cation, 24 cm^{-1} (observed). With the exception of C_{2h} symmetry *trans*-butene, all the equilibrium conformers have C_{2v} symmetry.
- (3) Cremer, D.; Binkley, J. S.; Pople, J. A.; Hehre, W. J. *J. Am. Chem. Soc.* **1974**, *96*, 6950.
- (4) Goodman, L.; Kundu, T.; Leszczynski, J. *J. Phys. Chem.* **1996**, *100*, 2770.
- (5) Pophrastic, V.; Goodman, L. *Nature* **2001**, *411*, 565.
- (6) Pophrastic, V.; Goodman, L. *J. Phys. Chem.* **2002**, *106*, 1642.
- (7) Senent, M. L.; Moule, D. C.; Smeyers, Y. G. *Can. J. Phys.* **1995**, *73*, 425.
- (8) Ozkabak, A. G.; Goodman, L. *Chem. Phys. Lett.* **1991**, *176*, 19.
- (9) Pophrastic, V.; Goodman, L. *J. Phys. Chem.* **2000**, *104*, 3231.
- (10) Senent, M. L.; Moule, D. C.; Smeyers, Y. G. *J. Chem. Phys.* **1995**, *102*, 5952.
- (11) Livingston, R. C.; Grant, D. M.; Pugmire, R. J.; Strong, K. A.; Brugger, R. M. *J. Chem. Phys.* **1973**, *58*, 1438.
- (12) Swalen, J. D.; Costain, C. C. *J. Chem. Phys.* **1959**, *31*, 1562.
- (13) Goodman, L.; Pophrastic, V. *Chem. Phys. Lett.* **1996**, *259*, 287.
- (14) Groner, P.; Durig, J. R. *J. Chem. Phys.* **1977**, *66*, 1856.
- (15) Myers, R. J.; Wilson, E. B. *J. Chem. Phys.* **1960**, *33*, 186.
- (16) Moller, K. D.; Andersen, H. G. *J. Chem. Phys.* **1962**, *37*, 1800.
- (17) Ozkabak, A. G.; Philis, J. G.; Goodman, L. *J. Am. Chem. Soc.* **1990**, *112*, 7854.
- (18) Pophrastic, V.; Goodman, L.; Guchhait, N. *J. Phys. Chem.* **1997**, *101*, 4290.
- (19) MP2/6-311G(3df,2p) energy calculation for C_{2v} symmetry geometrically restricted protonation, in which the proton is forced to stay in the molecular plane.
- (20) Goodman, L.; Pophrastic, V.; Weinhold, F. *Acc. Chem. Res.* **1999**, *32*, 983.
- (21) Pophrastic, V.; Goodman, L. *J. Chem. Phys.* **2001**, *115*, 5132.
- (22) Glendenning, E. D.; Badenhop, J. K.; Reed, A. E.; Carpenter, J. E.; Weinhold, F. NBO 4.M; Theoretical Chemistry Institute, University of Wisconsin: Madison, 1999.
- (23) Frisch, M. J.; G. H. Trucks; H. B. Schlegel; G. E. Scuseria; M. A. Robb; J. R. Cheeseman; V. G. Zakrzewski; J. A. Montgomery; R. E. Stratmann; J. C. Burant; S. Dapprich; J. M. Millam; A. D. Daniels; K. N. Kudin; M. C. Strain; O. Farkas; J. Tomasi; V. Barone; M. Cossi; R. Cammi; B. Mennucci; C. Pomelli; C. Adamo; S. Clifford; J. Ochterski; G. A. Petersson; P. Y. Ayala; Q. Cui; K. Morokuma; D. K. Malick; A. D. Rabuck; K. Raghavachari; J. B. Foresman; J. Cioslowski; J. V. Ortiz; B. B. Stefanov; G. Liu; A. Liashenko; P. Piskorz; I. Komaromi; R. Gomperts; R. L. Martin; D. J. Fox; T. Keith; M. A. Al-Laham; C. Y. Peng; A. Nanayakkara; C. Gonzalez; M. Challacombe; P. M. W. Gill; B. G. Johnson; W. Chen; M. W. Wong; J. L. Andres; M. Head-Gordon; E. S. Replogle; J. A. Pople, *Gaussian 98*; Gaussian, Inc.: Pittsburgh, PA, 1998.
- (24) Brunck, T. K.; Weinhold, F. *J. Am. Chem. Soc.* **1979**, *101*, 1700.
- (25) Groner, P., private communication.
- (26) Weinhold, F. Natural Bond Orbital Methods. In *The Encyclopedia of Computational Chemistry*; Schleyer, P. v. R., Allinger, N. L., Clark, T., Gasteiger, J., Kollman, P. A., Schaefer, H. F., III, Schreiner, P. R., Eds.; John Wiley & Sons: Chichester, 1998; Vol. 3; pp 1792–1811.
- (27) Badenhop, J. K.; Weinhold, F. *J. Chem. Phys.* **1997**, *107*, 5406.
- (28) Reed, A. E.; Curtiss, L. A.; Weinhold, F. *Chem. Rev.* **1988**, *88*, 899.
- (29) Unpublished work of the authors.